

Space-resolved photoluminescence of ZnS:Cu,Al nanocrystals fabricated by sequential ion implantation

Atsushi Ishizumi

Graduate School of Materials Science, Nara Institute of Science and Technology, Ikoma, Nara 630-0192, Japan

C. W. White

Solid State Division, Oak Ridge National Laboratory, Oak Ridge, Tennessee 37831

Yoshihiko Kanemitsu^{a)}

Graduate School of Materials Science, Nara Institute of Science and Technology, Ikoma, Nara 630-0192, Japan

(Received 1 December 2003; accepted 5 February 2004)

We report on photoluminescence (PL) properties of Cu- and Al-doped ZnS nanocrystals fabricated by sequential implantation of Zn⁺, S⁺, Cu⁺, and Al⁺ ions into Al₂O₃ matrices. The spatially resolved PL spectrum has been studied by a scanning near-field optical microscope (SNOM). In the SNOM image, bright spots are observed on the sample surface. The PL spectrum at each bright spot is broad and is not sensitive to the monitored positions. The broad SNOM-PL spectrum at each spot is very similar to the macroscopic PL spectrum measured by conventional optics. The donor-acceptor pair luminescence process in nanocrystals is discussed. © 2004 American Institute of Physics. [DOI: 10.1063/1.1689738]

Much interest has been focused on the fabrication and optical properties of semiconductor nanocrystals doped with luminescence centers, such as transition-metal and rare-earth ions,¹ since it is reported that Mn²⁺ doped ZnS nanocrystals show high photoluminescence (PL) efficiency and a short PL lifetime.² The doped nanocrystals have usually been fabricated by chemical synthesis methods.^{2,3} However, in the case of the doped nanocrystals fabricated by the chemical methods, it is suggested that doped ions are at the surface of nanocrystals.⁴ The luminescence properties depend on the surrounding chemical environment.³ On the other hand, it has been demonstrated that ion implantation is one of the most versatile methods for the fabrication of compound semiconductor nanocrystals embedded in transparent matrices.^{5,6} In particular, impurity-doped semiconductor nanocrystals can be simply fabricated by sequential ion implantation of the elements forming compound semiconductors and impurities.⁷

In this work, we have fabricated ZnS nanocrystals doped with Cu and Al (ZnS:Cu,Al nanocrystals) by ion implantation followed by thermal annealing, and have studied their PL properties. Spatially resolved PL spectra of individual ZnS:Cu,Al nanocrystals were measured by means of a scanning near-field optical microscope (SNOM). The donor-acceptor (DA) pair luminescence related to Cu and Al impurities is clearly observed in the nanocrystal samples. The spectral shape of the SNOM PL is very similar to that of the far-field PL measured by conventional optics. The origin of the broad PL spectrum of single ZnS:Cu,Al nanocrystals is discussed.

The *c*-axis oriented single crystal α -Al₂O₃ was used as a host material. Cu- and Al-doped ZnS nanocrystal samples

were fabricated by ion implantation of Zn⁺ ($1.0 \times 10^{17} \text{ cm}^{-2}$ at 420 keV), S⁺ ($1.0 \times 10^{17} \text{ cm}^{-2}$ at 225 keV), Cu⁺ (2.0×10^{15} or $1.0 \times 10^{16} \text{ cm}^{-2}$ at 400 keV), and Al⁺ (2.0×10^{15} or $1.0 \times 10^{16} \text{ cm}^{-2}$ at 170 keV) into the Al₂O₃ substrate, and then the samples were annealed at 1000 °C for 60 min in a flowing 96% Ar+4% H₂ atmosphere. Two samples with different impurity concentrations (but equal doses of Cu and Al ions) were prepared: the low-doped sample ($2.0 \times 10^{15} \text{ cm}^{-2}$) and the high-doped sample ($1.0 \times 10^{16} \text{ cm}^{-2}$). X-ray diffraction examination indicated that the ZnS nanocrystals are prepared as a mixture of hexagonal and cubic ZnS crystals.⁸

The far-field macro-PL spectra were measured under a 310 nm light excitation, using a cooled charge-coupled device (CCD) detector and a 32 cm monochromator. The spatially resolved PL spectra were measured by a SNOM system (JASCO, NFS-330). For the SNOM-PL measurements, the sample was illuminated with 325 nm He–Cd laser light through an aperture of fiber probe with a pure-SiO₂ core. The PL signals from the sample were collected by the same aperture (a so-called illumination and collection mode) and detected by a cooled CCD detector through a 25 cm monochromator. The spectral sensitivity of the measuring system was also calibrated using a tungsten standard lamp.

Figure 1 shows macro-PL, PL excitation, and absorption spectra of (a) the low-doped and (b) the high-doped samples at 14 K. In the low-doped sample, four peaks are clearly observed in the absorption spectrum, and their peak energies are indicated by the arrows in Fig. 1(a). It is found that the energies of the four peaks almost coincide with the exciton energy (3.81 eV) in the cubic ZnS bulk crystal and the A, B, and C exciton energies (3.88, 3.90, and 3.98 eV) in the hexagonal ZnS bulk crystal, respectively.⁹ This result shows that the ZnS nanocrystal sample is a mixture of cubic and hexagonal ZnS crystals, and this observation is consistent with x-ray diffraction examination.⁸ The broad PL band is ob-

^{a)} Author to whom correspondence should be addressed; present address: Institute for Chemical Research, Kyoto University, Uji, Kyoto 611-0011, Japan; electronic mail: kanemitu@scl.kyoto-u.ac.jp

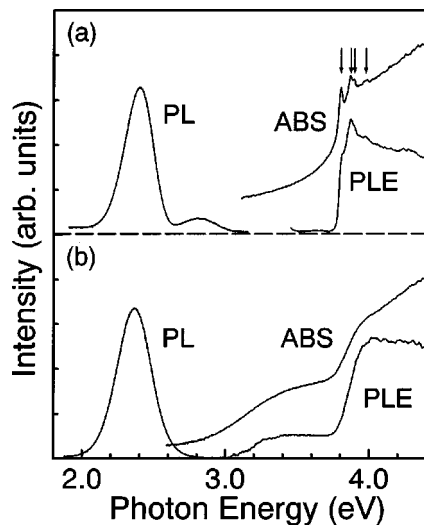


FIG. 1. PL, PL excitation, and optical absorption spectra of (a) the low-doped sample and (b) the high-doped sample at 14 K.

served around 2.40 eV, similar to the intense green luminescence of ZnS:Cu,Al bulk crystals.^{10,11} In undoped ZnS nanocrystal samples, the broad green PL is not observed. Therefore, it is believed that the broad PL spectrum in ZnS:Cu,Al nanocrystals is ascribed to the DA pair (Al–Cu pair) luminescence in ZnS.

In the high-doped sample, the broad PL band is observed around 2.40 eV, as shown in Fig. 1(b). In the PL excitation and absorption spectra, the hump around 3.4 eV was observed, in addition to the band-to-band transition of ZnS nanocrystals around 4 eV. A similar hump is observed in the PL excitation spectrum of ZnS:Cu,Al bulk crystals and this is assigned to the transition of an electron from the Cu acceptor to the conduction band.¹² The PL intensity of the high-doped sample [Fig. 1(b)] is much larger than that of the low-doped sample [Fig. 1(a)]. The doped impurities control the optical absorption and luminescence properties of ZnS:Cu,Al nanocrystals. The average size of ZnS nanocrystals in the high-doped sample is estimated to be 10 nm, from the blueshift of the peak energy of the PL excitation spectrum.

Figure 2(a) shows the spatial profiles of the spectrally

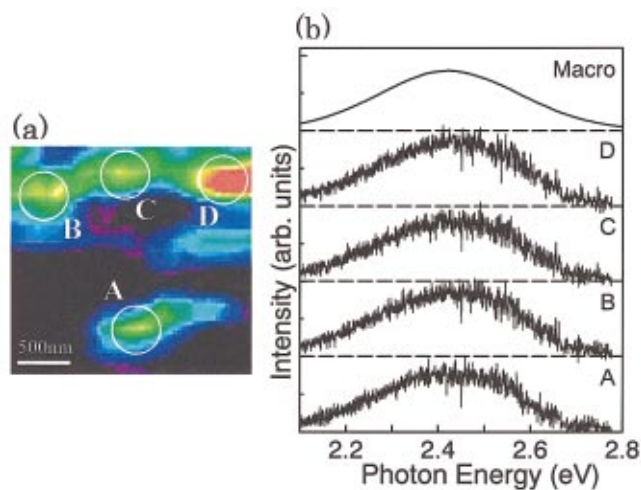


FIG. 2. (Color) (a) Two-dimensional SNOM-PL image of the high-doped sample at room temperature. (b) SNOM-PL spectra at different bright spots and the macro-PL spectrum at room temperature.

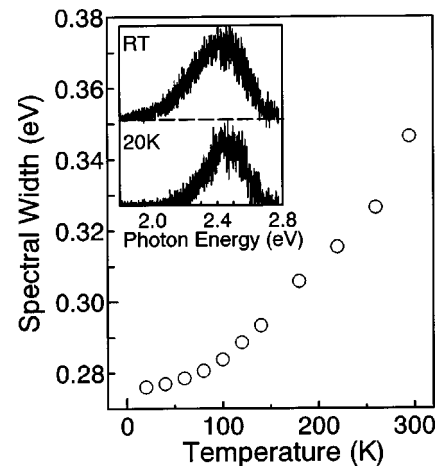


FIG. 3. Temperature dependence of the spectral width (full width at half maximum) in the macro-PL. The inset shows the SNOM-PL spectra at room temperature and at 20 K.

integrated PL intensity of the high-doped sample at room temperature. Several bright spots are observed on the sample surface and these correspond to the light-emitting ZnS:Cu,Al nanocrystals. The spectra of SNOM PL at several bright points are shown in Fig. 2(b). It is found that the peak energy and spectral width of the SNOM PL at each position almost coincide. Furthermore, the observed SNOM-PL spectrum is very similar to the macro-PL one. These results are completely different from the PL properties of shallow impurities in CdS nanocrystals fabricated by ion implantation.¹³ In CdS nanocrystals, sharp PL lines are observed in the SNOM-PL spectrum, and the shallow impurity PL spectrum is very sensitive to the monitored position under the same experimental condition.¹⁴ The broad PL band in the macro-PL spectrum consists of an assembly of sharp PL lines of individual nanocrystals.¹³ On the other hand, in ZnS:Cu,Al nanocrystals, the sharp PL lines cannot be observed in the SNOM-PL spectrum and the PL spectrum of a single ZnS:Cu,Al nanocrystal is very broad. Rather, the SNOM-PL spectrum is very similar to the macro-PL spectrum. In order to clarify the origin of the broad PL spectrum from single nanocrystals, we have studied PL spectra as a function of the excitation laser intensity and the measurement temperature.

The inset of Fig. 3 shows the SNOM-PL spectra of the high-doped ZnS:Cu,Al nanocrystal sample at room temperature and at 20 K. Even at 20 K, the observed spectrum was the broad Gaussian shape. The spectral width of the SNOM-PL band at room temperature is larger than that at 20 K. In addition, the spectral width of the macro-PL band (full width at half maximum) is plotted as a function of the measurement temperature in Fig. 3. The spectral width of the green PL increases with an increase of temperature. Both macro-PL and SNOM-PL are sensitive to the measurement temperature. In addition, the spectral widths of the SNOM-PL at room temperature and at 20 K are almost the same as that of the macro-PL. These observations imply that the macro-PL spectrum is mainly determined by the luminescence processes in single nanocrystals, rather than the broad size distribution of the nanocrystals in the sample. Since the level of the Cu acceptor is known to have a binding energy of about 1.20 eV,¹⁵ the spectrum of a single DA pair luminescence is expected to be very narrow. However, the observed macro-PL spectrum is very broad. This broad PL spectrum is mainly determined by the luminescence processes in single nanocrystals, rather than the broad size distribution of the nanocrystals in the sample. Since the level of the Cu acceptor is known to have a binding energy of about 1.20 eV,¹⁵ the spectrum of a single DA pair luminescence is expected to be very narrow. However, the observed macro-PL spectrum is very broad. This broad PL spectrum is mainly determined by the luminescence processes in single nanocrystals, rather than the broad size distribution of the nanocrystals in the sample.

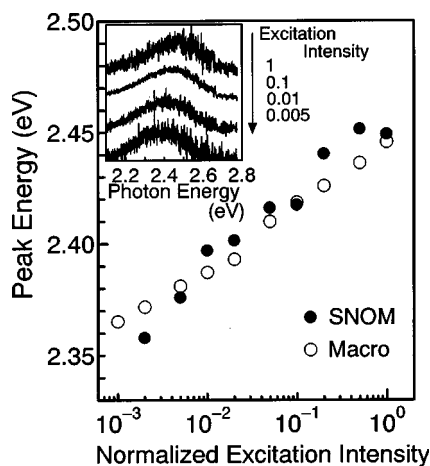


FIG. 4. Excitation intensity dependence of the peak energy in the SNOM-PL (closed circles) and the macro-PL spectra (open circles) of ZnS:Cu,Al nanocrystals at 20 K. Similar excitation intensity dependence is observed in the SNOM-PL and the macro-PL spectra. The inset shows the SNOM-PL spectra at different excitation intensities.

nescence is broadened by the strong interaction between phonons and the electrons trapped at the deep Cu acceptors.

The inset of Fig. 4 shows the SNOM-PL spectra under different laser intensity excitation at 20 K. The peak energy of the SNOM-PL spectrum shifts to higher energy with an increase of the excitation laser intensity. In Fig. 4, the PL peak energies of the SNOM-PL and macro-PL spectra are plotted as a function of the excitation intensity at 20 K. Similar excitation intensity dependence of the PL peak energy is observed in the SNOM-PL and macro-PL spectra. These observations in Figs. 3 and 4 show that the broad PL is due to the DA pair luminescence processes in ZnS:Cu,Al nanocrystals.

In the DA pair recombination process, the emission photon energy depends on the distance R between donors and acceptors, and is given by^{15,16}

$$E = E_g - E_A - E_D + e^2/\epsilon R,$$

where E_g is the band-gap energy, E_D and E_A are the donor and acceptor binding energies and ϵ is the static dielectric constant. Under high intensity excitation, almost all donors and acceptors are neutralized. The DA pair luminescence is dominated by the recombination of closer pairs, having large recombination probability and emitting higher energy photons.¹⁶ On the other hand, under low intensity excitation, the number of neutralized donors and acceptors decreases: The contribution of the recombination of distant pairs, having small recombination probability, appears in the DA pair luminescence. The energy of photons emitted by the recombination of distant pairs is lower than that of closer pairs. Therefore, in the DA pair luminescence, the peak energy of the PL spectrum shifts to a lower energy with a decrease of the excitation intensity, as shown in Fig. 4.

In ZnS:Cu,Al, the Al donor has a shallow level with the binding energy of about 0.10 eV, and the Bohr radius is 1.2 nm,¹⁷ while the binding energy of the Cu acceptor is about 1.20 eV. In ZnS:Cu,Al nanocrystals, the acceptor Bohr radius is negligibly small compared to the donor Bohr radius. Therefore, the probability of the DA-pair recombination P depends on the distance R between the donors and acceptors

and the donor Bohr radius a_D ; $P \propto \exp[-2R/a_D]$. In our samples, the average diameter of the high-doped sample (about 10 nm) is larger than the extent of the wave function of the electron trapped at donors (1.2 nm). When there exist many Al and Cu impurities in a single nanocrystal, the PL spectrum consists of an assembly of the PL bands due to the recombination of various DA pairs. Then, the PL spectrum of single nanocrystals is sensitive to the excitation intensity, similar to the case of bulk ZnS:Cu,Al crystals. In our sample, the macro-PL spectrum is mainly determined by the spectral broadening mechanism in a single nanocrystal (the strong electron-phonon interaction and the distribution of the DA pair distance in a single nanocrystal), rather than the broad size distribution of the nanocrystals in the sample.

In conclusion, we have studied the optical properties of Cu- and Al-doped ZnS nanocrystals formed by sequential Zn⁺, S⁺, Cu⁺, and Al⁺ ion implantation into Al₂O₃ matrices. The DA pair luminescence related to Cu and Al impurities is clearly observed in Cu- and Al-doped ZnS nanocrystals. The PL spectrum in a single ZnS:Cu,Al nanocrystal is broadened by the strong electron-phonon coupling and the distance distribution between donors and acceptors. Our spectroscopic data show that sequential ion implantation is a unique method for synthesizing nanoparticles doped with optically active impurities.

Part of this work at Nara was supported by a Grant-in-Aid for Scientific Research (KAKENHI, 14340093) from the Japan Society for the Promotion of Science. Oak Ridge National Laboratory is managed by UT-Battelle, LLC for the U.S. Department of Energy under Contract No. DE-AC05-00OR22725.

- ¹ See, for example, L. E. Brus, Al. L. Efros, and T. Itoh, *J. Lumin.* **70**, 1 (1996).
- ² R. N. Bhargava, D. Gallagher, X. Hong, and A. Nurmikko, *Phys. Rev. Lett.* **72**, 416 (1994).
- ³ A. A. Bol and A. Meijerink, *Phys. Rev. B* **58**, R15997 (1998); *Phys. Status Solidi B* **224**, 291 (2001).
- ⁴ P. H. Borse, D. Srinivas, R. F. Shinde, S. K. Date, W. Vogel, and S. K. Kulkarni, *Phys. Rev. B* **60**, 8659 (1999).
- ⁵ C. W. White, J. D. Budai, S. P. Withrow, J. G. Zhu, E. Sonder, R. A. Zuhr, A. Meldrum, D. M. Hembree, Jr., D. O. Henderson, and S. Prawer, *Nucl. Instrum. Methods Phys. Res. B* **141**, 228 (1998).
- ⁶ Y. Kanemitsu, H. Tanaka, T. Kushida, K. S. Min, and H. A. Atwater, *Phys. Rev. B* **62**, 5100 (2000).
- ⁷ Y. Kanemitsu, H. Matsubara, and C. W. White, *Appl. Phys. Lett.* **81**, 535 (2002).
- ⁸ A. Meldrum, E. Sonder, R. A. Zuhr, I. M. Anderson, J. D. Budai, C. W. White, L. A. Boatner, and D. O. Henderson, *J. Mater. Res.* **14**, 4489 (1999).
- ⁹ *Semiconductors Physics of Group II-VI Compounds*, Ländolt-Börnstein, New Series, Group III, Vol. 17, edited by O. Madelung, M. Schulz, and H. Weiss, Pt. b (Springer, Berlin, 1982).
- ¹⁰ K. Era, S. Shionoya, and Y. Washizawa, *J. Phys. Chem. Solids* **29**, 1827 (1968).
- ¹¹ K. Era, S. Shionoya, Y. Washizawa, and H. Ohmatsu, *J. Phys. Chem. Solids* **29**, 1843 (1968).
- ¹² A. Suzuki and S. Shionoya, *J. Phys. Soc. Jpn.* **31**, 1455 (1971).
- ¹³ M. Ando, Y. Kanemitsu, T. Kushida, K. Matsuda, T. Saiki, and C. W. White, *Appl. Phys. Lett.* **79**, 539 (2001).
- ¹⁴ A. Ishizumi, C. W. White, and Y. Kanemitsu (unpublished).
- ¹⁵ *Phosphor Handbook*, edited by S. Shionoya and W. M. Yen (CRC, Boca Raton, FL, 1999).
- ¹⁶ See, for example, P. Y. Yu and M. Cardona, *Fundamentals of Semiconductors* (Springer, Berlin, 1996).
- ¹⁷ H. Kukimoto, S. Shionoya, T. Koda, and R. Hioki, *J. Phys. Chem. Solids* **29**, 935 (1968).